DNA-Programmed Assembly

DOI: 10.1002/anie.201000633

Establishing the Design Rules for DNA-Mediated Programmable Colloidal Crystallization**

*Robert J. Macfarlane, Matthew R. Jones, Andrew J. Senesi, Kaylie L. Young, Byeongdu Lee, Jinsong Wu, and Chad A. Mirkin**

In 1996, we introduced the concept of using DNA and its programmable recognition properties to guide the assembly of polyvalent DNA nanoconjugates into macroscopic materials.[1] Over the past decade, we[3–7] and others[2,8-10] have developed methods for using DNA nanoconjugates to realize ordered arrangements of small clusters and highly crystalline extended architectures. Through this work, we have begun to define the design rules for synthesizing nanoparticle structures from DNA where one can envision and realize a particle lattice through the appropriate use of nanoparticle and DNA building blocks. In principle, the approach lends itself to many particle sizes and different lengths of DNA interconnects, thereby providing a new construction kit for realizing a wide array of nanoparticle-based three-dimensional architectures. The ability to assemble crystalline lattices with control over both nanoparticle size and interparticle distance would represent a major advance for nanotechnology, as the physical properties of nanomaterials are highly dependent upon both their size and surrounding environment.[11–15] However, changing the dimensions of nanomaterials used in the assembly process also alters the manner in which the materials behave by changing the relative magnitudes and types of fundamental forces driving assembly. As such, design rules need to be established that take these differences into account to develop a complete understanding of DNA-based particle assembly. Herein, we report a set of experiments that demonstrate that there are predictable and mathematically definable relationships between particle size and DNA length that dictate the assembly and crystallization processes. These experiments allow us to define a "zone of crystallization", wherein we can understand, explain, and control the biomolecular forces driving the formation of colloidal crystals with programmable variation of both crystal lattice parameters and nanoparticle size.

Gold nanoparticles (AuNPs) of approximately 5–80 nm in diameter were densely functionalized with alkylthiol-modified oligonucleotides according to established procedures.[16] (All DNA sequences can be found in the Supporting Information.) DNA linker strands were then added to these DNA-functionalized AuNPs to induce AuNP aggregation (Figure 1b). The 3′ end of each linker contained an 18-mer sequence complementary to the 3′ end of the AuNP-bound DNA, while the 5′ end contained a short, self-complementary 5′-CGCG-3′ sequence that induced particle aggregation.

To vary the length of the DNA linkers (and thereby control the distance between nanoparticles in an aggregate), a spacer sequence, consisting of modular "blocks" of a repeated 40-base DNA segment, was placed in-between the particle-recognition sequence and the 5′-CGCG-3′ sequence. DNA length was controlled by varying the number of blocks in each linker strand. We have previously determined that there is an approximate 0.255 nm rise per base pair for the DNA linkers, meaning that each block adds approximately 10 nm to the overall length of a single DNA strand.[4] Each of these sections (particle recognition sequence, 5′-CGCG-3′ sequence, and each individual block spacer) was separated by a single unpaired "flexor" base, which has been shown to be important in the formation of DNA-AuNP crystals.[3–5] A 40-base DNA strand complementary to the block region (added in a 1:1 ratio with the number of blocks in the linker strand's sequence) was hybridized to the linker strands prior to combining them with the DNA-AuNPs. This was done both to increase linker rigidity and to make this design conform with previously established crystallization schemes.[3–5] DNA-AuNPs were crystallized by adding linkers to the nanoparticle solutions and heating the resulting aggregates to a few

[*] R. J. Macfarlane, A. J. Senesi, K. L. Young, Prof. C. A. Mirkin
Department of Chemistry, Northwestern University
2190 Campus Drive, Evanston, IL 60201 (USA)
Fax: (+1) 847-491-7713
E-mail: chadnano@northwestern.edu
M. R. Jones, J. Wu, Prof. C. A. Mirkin
Department of Materials Science & Engineering
Northwestern University
2190 Campus Drive, Evanston, IL 60201 (USA)
B. Lee
X-ray Science Division, Argonne National Laboratory (USA)

[**] We acknowledge George Schatz for helpful discussions regarding the theoretical calculations of DNA flexibility and relative DNA concentrations in aggregates. C.A.M. acknowledges the NSF-NSEC and the AFOSR for grant support. He also is grateful for a NIH Director's Pioneer Award and an NSSEF Fellowship from the DoD. Portions of this work were supported as part of the Non-Equilibrium Energy Research Center (NERC), an Energy Fontier Research Center funded by the U.S. Department of Energy, Office of Science, Office of Basic Energy Sciences under Award Number DE-SC0000989. R.J.M. acknowledges Northwestern University for a Ryan Fellowship. M.R.J. acknowledges Northwestern University for a Ryan Fellowship and the NSF for a Graduate Research Fellowship. K.L.Y. acknowledges the NSF and the NDSEG for Graduate Research Fellowships. Portions of this work were performed at the DuPont-Northwestern-Dow Collaborative Access Team (DND-CAT) located at Sector 5 of the Advanced Photon Source (APS). DND-CAT is supported by E.I. DuPont de Nemours & Co., The Dow Chemical Company, and the State of Illinois. Use of the APS was supported by U.S. Department of Energy, Office of Science, Office of Basic Energy Sciences, under Contract No. DE-AC02-06CH11357.

Supporting information for this article is available on the WWW under http://dx.doi.org/10.1002/anie.201000633.

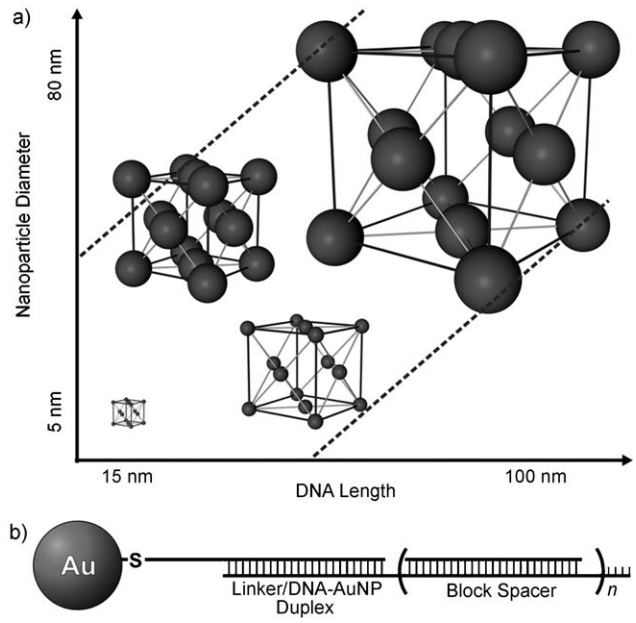

Figure 1. Programmable assembly of nanoparticles. a) The lattice parameters of DNA-programmed colloidal crystals are tunable by both DNA length and nanoparticle size within a "zone of crystallization" (in between the dashed lines), as defined by the ratio of nanoparticle diameter to linking DNA length. b) The DNA design that links nanoparticles together, consisting of: a hexylthiol moiety, a dA_{10} spacer, a particle–linker duplex, a series of "block" spacers (where $n = 0$–4), and a short, self-complementary linker–linker recognition sequence.

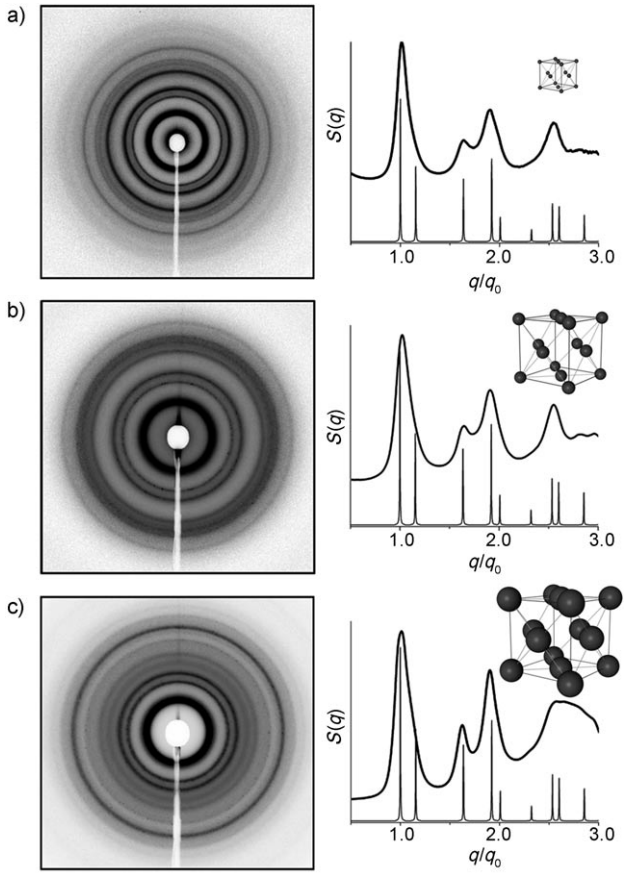

Figure 2. The 1D and 2D SAXS patterns for crystals consisting of a) 10.4 nm AuNPs, unit cell edge length 67.4 nm; b) 31.3 nm AuNPs, unit cell edge length 151 nm; and c) 60.9 nm AuNPs, unit cell edge length 183 nm. (Due to the exponential decay of X-ray scattering as a function of scattering vector, the contrast of the 2D SAXS image in (c) was adjusted nonlinearly. This did not affect the 1D plot or data analysis.)

degrees below their melting temperature (the temperature at which the DNA-AuNPs would dissociate).

Face-centered cubic (fcc) colloidal crystals were obtained with control over nanoparticle components and lattice parameters on a diverse length scale. The nanoparticle sizes range from 5 to almost 80 nm in diameter (Figure 2; Supporting Information, Figure S1–S8), and the unit cell edge lengths of the crystals range from about 25 to 225 nm. Resulting crystal sizes varied, with the average domain size being 1.5 μm in diameter, corresponding to 10^2–10^5 AuNPs/crystal, depending on unit cell dimensions (Supporting Information, Table S4), and the largest crystal being approximately 2.6 μm in diameter.

All of the calculated lattice parameters for these crystals are within approximately 10% of predicted values[4]—most of the systems deviate from prediction by less than 5%, indicating that the crystal lattice parameters are tailorable over the entire size regime studied and that the unit cell edge lengths can be predicted using our previous model.[4] Furthermore, the lattice parameters can be moderately controlled by changes in solution temperature, as they were controllably and reversibly expanded by as much as 8% with only a 20°C increase in temperature (Supporting Information, Figure S10). Because the DNA sequences used to assemble NPs have synthetically variable numbers of base pairs connecting them, each of which contributes 0.255 nm to the distance between nanoparticles, this gives us nanometer-scale precision over the assembled crystal structures.

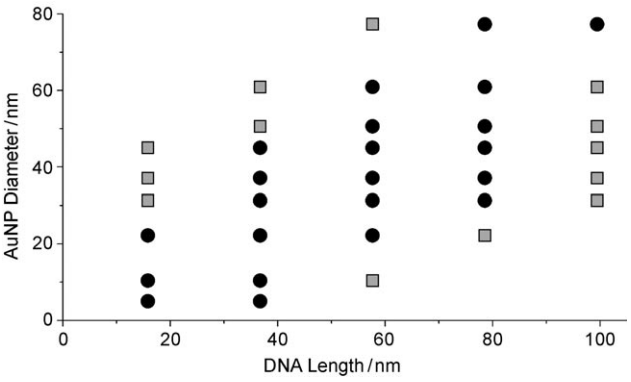

Figure 3. The zone of crystallization, as defined by the relationship between nanoparticle diameter and DNA length. Black circles indicate that fcc crystals were formed, and gray squares indicate that only disordered aggregates were observed.

Significantly, not all of the DNA-linker and AuNP combinations we designed formed well-defined crystal structures (Figure 3). Indeed, the data can be clearly delineated

into three distinct realms in which the total DNA length is significantly longer, of comparable length, or significantly shorter than the nanoparticle diameter—only the middle region leads to well-formed crystalline aggregates. The boundaries of this zone of crystallization are of fundamental interest, as they allow for explanation of the DNA behavior that leads to ordered nanoparticle assemblies.

The fact that crystals are not formed at low DNA length to AuNP diameter ratios (gray squares, upper left of Figure 3) can be understood by making a comparison between the polydispersity of the AuNPs and the flexibility of the DNA strands (Figure 4a). Double-stranded DNA exhibits length-dependent flexibility with a persistence length of approximately 50 nm.[17] Thus, longer DNA linkers have greater variation in the distance between the AuNP surface and the 5′-CGCG-3′ recognition units (ΔL; Figure 4a). The data (Figure 4b; calculations can be found in the Supporting Information) show that crystals form in systems where the values of ΔL are equivalent to or greater than the variability in nanoparticle size (ΔD, calculated as the size polydispersity of a given NP solution), but not when the opposite is true. In a system in which particle size dispersity is greater than DNA flexibility, a well-ordered crystal is no longer the most thermodynamically favorable state. We project that this is because the energetic penalties associated with the DNA stretching and/or bending to direct the assembly of non-uniform AuNPs into a uniform lattice are too great to provide significant net enthalpic energy benefit.[17,18]

This thermodynamic trade-off does not, however, explain the upper limit to the length of DNA strands that can be used for each nanoparticle size (gray squares, bottom right of Figure 3). Longer DNA linkers, with their increased flexibility, would not suffer the enthalpic penalties mentioned above, indicating that the limiting factor for crystal formation with longer DNA lengths may be kinetic rather than thermodynamic. To form an ordered crystal, the DNA ligands holding nanoparticles together must go through a process of de- and re-hybridization to transition from an initially disordered structure to their most ordered crystalline state.[5,19] The rate at which these binding events occur can be defined by a k_{on} and k_{off} for the DNA ligands, where maximum rearrangement occurs when the values of k_{on} and k_{off} are both high, but $k_{on} > k_{off}$. The weak, polyvalent nature of the DNA-AuNP hybridization scheme is critical for this reorganization process, as the weak binding of individual linker recognition units allows for high values of k_{off}, while the high local concentration of DNA on the surface of the nanoparticles inflates the values of k_{on}. The combined effect of these high k_{on} and k_{off} rates results in "mobile" nanoparticles within an aggregate, where repositioning of the DNA-AuNPs is possible.

To determine the relative k_{on} and k_{off} values for these nanoparticle systems, an effective concentration (C_{eff}) for the DNA linker recognition units within an aggregate was determined (for calculations, see the Supporting Information). C_{eff} is defined as the number of linker recognition units per particle divided by the limited volume in which they exist, due to localized confinement

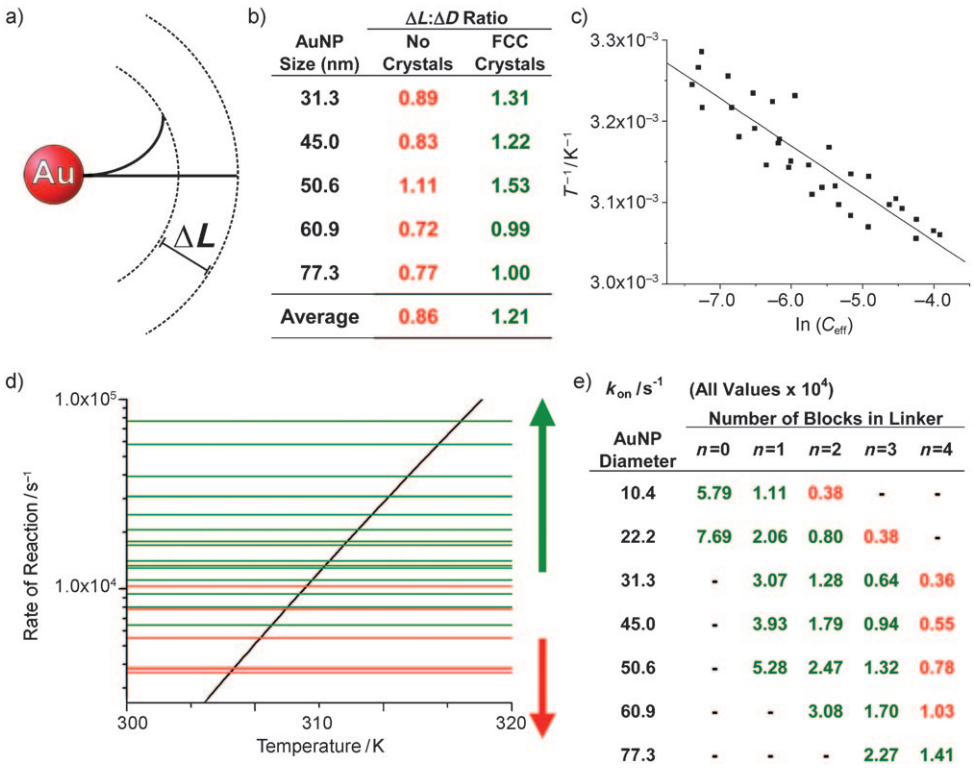

Figure 4. Differences in nanoparticle size and DNA length govern the crystal formation process. a) The distance between the AuNP surface and the linker recognition unit shows variability as a function of the length of the DNA strand (ΔL). b) The ratios of ΔL versus variability in nanoparticle size (ΔD) for the longest DNA length in which fcc crystals were not observed (data from gray squares, upper left of Figure 3) and the shortest DNA length in which they were (data from black circles, upper left of Figure 3). In general, ordered assemblies are only obtained when $\Delta L \geq \Delta D$. c) A plot of $1/T_m$ values against $\ln(C_{eff})$ for each DNA-AuNP system shows that the data follow a linear trend. The value of ΔH of hybridization calculated from this plot is within 6.7% of a previously published value for the non-AuNP-bound 5′-CGCG-3′ duplex. d) The k_{on} values for crystalline (green traces) and noncrystalline (red traces) DNA-AuNP aggregates, demonstrating that only DNA-AuNPs with high values of k_{on} are able to form crystals. The value of k_{off} is plotted as a function of temperature (black trace). e) When the k_{on} values are large enough (green values), the system can reach temperatures high enough to allow for reorganization of the DNA-AuNPs within an aggregate. However, DNA-AuNP systems with relatively low k_{on} values (red values) melt at temperatures too low to allow the AuNPs to form an ordered crystal.

of DNAs tethered to the surface of a AuNP. Values of $1/T_m$ were plotted against values of $\ln(C_{eff})$, where T_m is the temperature at which an aggregate dissociates. These values exist in a linear relationship (Figure 4c) and can be used to determine the thermodynamic constants ($\Delta H°$ and $\Delta S°$) associated with DNA duplex formation. Based on the data calculated in Figure 4c, the $\Delta H°$ value for DNA hybridization is $-141.9\ kJ\,mol^{-1}$, which is within 6.7% variance from previously established literature values for this 5′-CGCG-3′ sequence,[19] indicating that this is indeed an accurate model.

Using these data, plots of calculated k_{on} and k_{off} values show reasonable agreement with experimental T_m values for the systems studied. When the k_{on} of a system is less than $6\times10^3\ s^{-1}$, no crystals are observed. This indicates that, at the temperatures immediately below dehybridization of the linker–linker overlap for these systems, there is not enough thermal energy to induce restructuring of the nanoparticles on an appreciable timescale. However, when the k_{on} of a system is greater than $1\times10^4\ s^{-1}$, the rates of DNA de- and re-hybridization are fast enough to induce restructuring in the aggregate at temperatures slightly below T_m. (Between these values, some systems are able to restructure, while others are not; these data are discussed in more detail in the Supporting Information.) These kinetic data explain the results at the bottom right of Figure 3, where systems with large DNA length to AuNP diameter ratios are unable to transition from disordered aggregates to ordered crystals—it is in these systems that the lowest rates of k_{on} are observed.

In conclusion, we have determined that there is a definable relationship between DNA length and particle size in the DNA-directed assembly of nanoparticles. This discovery enables not only a better understanding of the fundamental forces driving the crystallization process, but also the formation of colloidal crystals with tailorable features, including interparticle distance, particle size, degree of filled space, and unit cell lattice parameters. The method we have developed to model DNA strands constrained on surfaces of NPs and predict their assembly behavior provides a basis for future exploration into the interactions of DNA and nanoscale objects, and we project that these methods can be extended to studies of nanoparticles with different shapes and compositions. These discoveries will serve as a template for future nanoparticle crystallization efforts, allowing for the formation of crystals with controllable and tunable physical properties.

Received: February 2, 2010
Published online: May 18, 2010

Keywords: colloidal crystals · DNA · nanomaterials

[1] C. A. Mirkin, R. L. Letsinger, R. C. Mucic, J. J. Storhoff, *Nature* **1996**, *382*, 607.
[2] A. P. Alivisatos, K. P. Johnsson, X. G. Peng, T. E. Wilson, C. J. Loweth, M. P. Bruchez, P. G. Schultz, *Nature* **1996**, *382*, 609.
[3] S. Y. Park, A. K. R. Lytton-Jean, B. Lee, S. Weigand, G. C. Schatz, C. A. Mirkin, *Nature* **2008**, *451*, 553.
[4] H. D. Hill, R. J. Macfarlane, A. J. Senesi, B. Lee, S. Y. Park, C. A. Mirkin, *Nano Lett.* **2008**, *8*, 2341.
[5] R. J. Macfarlane, B. Lee, H. D. Hill, A. J. Senesi, S. Seifert, C. A. Mirkin, *Proc. Natl. Acad. Sci. USA* **2009**, *106*, 10493.
[6] J. J. Storhoff, A. A. Lazarides, R. C. Mucic, C. A. Mirkin, R. L. Letsinger, G. C. Schatz, *J. Am. Chem. Soc.* **2000**, *122*, 4640.
[7] S. Y. Park, J.-S. Lee, D. Georganopoulou, C. A. Mirkin, G. C. Schatz, *J. Phys. Chem. B* **2006**, *110*, 12673.
[8] D. Nykypanchuk, M. M. Maye, D. van der Lelie, O. Gang, *Nature* **2008**, *451*, 549.
[9] H. Xiong, D. van der Lelie, O. Gang, *Phys. Rev. Lett.* **2009**, *102*, 015504.
[10] W. Cheng, M. R. Hartman, D.-M. Smilgies, R. Long, Michael J. Campolongo, R. Li, K. Sekar, C.-Y. Hui, D. Luo, *Angew. Chem. Int. Ed. Angew. Chem.* **2009**, *121*, 6587; *Angew. Chem. Int. Ed. Engl.* **2009**, *48*, 6465.
[11] A. P. Alivisatos, *Science* **1996**, *271*, 933.
[12] B. Nikoobakht, M. A. El-Sayed, *Chem. Mater.* **2003**, *15*, 1957.
[13] K. L. Kelly, E. Coronado, L. L. Zhao, G. C. Schatz, *J. Phys. Chem. B* **2003**, *107*, 668.
[14] J. E. Millstone, G. S. Métraux, C. A. Mirkin, *Adv. Funct. Mater.* **2006**, *16*, 1209.
[15] W. S. Seo, H. H. Jo, K. Lee, B. Kim, S. J. Oh, J. T. Park, *Angew. Chem.* **2004**, *116*, 1135; *Angew. Chem. Int. Ed.* **2004**, *43*, 1115.
[16] H. D. Hill, C. A. Mirkin, *Nat. Protoc.* **2006**, *1*, 324.
[17] C. Rivetti, C. Walker, C. Bustamante, *J. Mol. Biol.* **1998**, *280*, 41.
[18] J. SantaLucia, D. Hicks, *Annu. Rev. Biophys. Biomol. Struct.* **2004**, *33*, 415.
[19] S. M. Freier, N. Sugimoto, A. Sinclair, D. Alkema, T. Neilson, R. Kierzek, M. H. Caruthers, D. H. Turner, *Biochemistry* **1986**, *25*, 3214.

